SLAC PUB 5215
April 1990
(A/E)

A NEW TARGET DESIGN AND CAPTURE STRATEGY FOR HIGH-YIELD POSITRON PRODUCTION IN ELECTRON LINEAR COLLIDERS *

MARY JAMES†, RICK DONAHUE, ROGER MILLER AND W. R. NELSON

Stanford Linear Accelerator Center
Stanford University, Stanford, California 94309

Abstract

Monte Carlo calculations were performed using EGS4 to simulate the production of positrons by a high energy electron beam incident on thin wire targets. A one mm diameter, ten radiation length long tungsten-alloy wire was chosen as an optimal target. The new target, combined with an appropriate capture strategy, could triple the yield of the high energy positron production systems currently in use.

Submitted to Nuclear Instruments and Methods.

---

* Work supported by the US Department of Energy under contract DE-AC03-76SF00515

† PRESENT ADDRESS: *Physics Department, Reed College, Portland, Oregon*

1. Introduction

Positron beams at high-energy accelerators are produced in an electromagnetic cascade shower initiated by a high-energy electron beam incident on high-Z target material. To maximize positron yield, the thickness of the target is chosen to be equal to shower maximum in the target material. Simulations of the electromagnetic shower reveal that large numbers of low-energy positrons are produced as the shower progresses. Most of these low-energy positrons are reabsorbed before reaching the downstream edge of the target. Present targets have transverse dimensions on the order of 1 cm. In this paper we examine the possibility of using a small diameter "wire" target in order to allow positrons to emerge from the sides, thereby avoiding reabsorption. A different capture strategy[1] designed to maximize the capture of positrons emitted from the proposed wire target is also presented.

2. Positron Yields From A Wire Target

The EGS4 Code System[2] was used to simulate positron production in tungsten wires of varying diameters. The model assumed a 33 GeV electron beam incident on a 6 radiation length wire. Figure 1 shows positron yields in the energy range of 5 to 20 MeV* for tungsten (and uranium) wires with radii ranging from 0.001 to 1 cm. The yields are normalized to the calculated yield from a 6 r.l. semi-infinite slab of tungsten, which reasonably approximates the present SLC positron target.

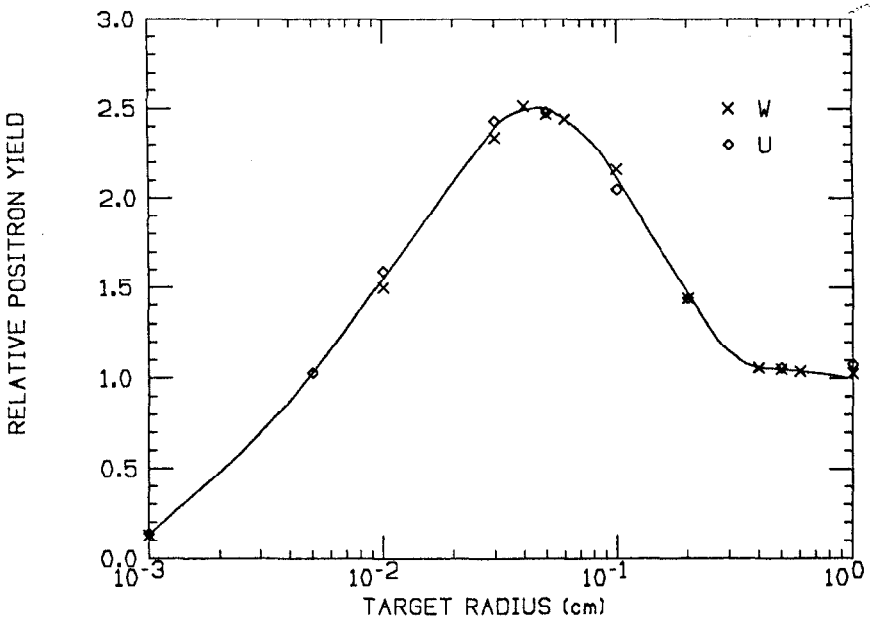

Figure 1. Yield of 5 to 20 MeV positrons from 6 r.l. wires as a function of radius (normalized to the yield from a 6 r.l. semi-infinite tungsten target).

---

* This energy range is consistent with the current SLC target-collector system.

Yield is defined as any positron that ultimately passes through the plane of the downstream end of the target, regardless of its distance from the central axis, its transverse momentum, or its arrival time at the plane† .

At very small wire radii, high-energy charged particles and photons escape from the sides of the wire, precluding the development of a substantial electromagnetic cascade. At large wire radii the shower reaches maximum development, but many of the low-energy positrons are reabsorbed before reaching the downstream edge of the target. Figure 1 suggests that the maximum positron yield will be obtained with a 1 mm diameter wire. This yield is found to be 2.5 times greater than that achieved by similar EGS4 calculations for the present SLC positron source[3], the increase due to particles emerging from the sides of the target.

After fixing the diameter of the tungsten wire to 1 mm, we simulated positron production in wires of varying lengths surrounded by vacuum, beryllium and carbon. Figure 2 shows the positron yield for wire targets ranging from 5 to 10 r.l. The curves have again been normalized to the yield obtained with a 6 r.l. semi-infinite slab of tungsten chosen to approximate the geometry of the current SLC target.

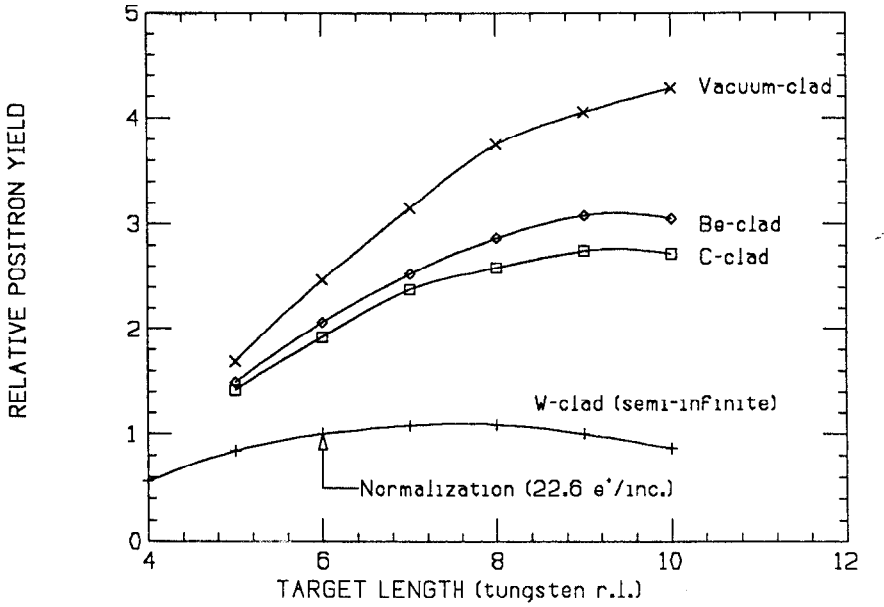

Figure 2. Positron yield vs. target length for 1 mm diameter tungsten wires clad with various materials (5 to 20 MeV).

As the figure shows, a yield of almost 100 positrons per electron can be achieved using a 10 r.l. wire suspended in vacuum—a factor of 4.3 increase over the 6 r.l. infinite slab target.

Since most of the increased yield is due to low-energy positrons emerging from the sides of the wire, we now turn our attention to the question of whether these positrons can be captured, accelerated and successfully injected into the SLC.

---

† EGS4 was modified to include time as a particle property.

3. Positron Capture and Acceleration

The present SLC positron source is shown schematically in Figure 3. A beam of 33 GeV electrons is incident from the left upon a 0.6 cm radius, 2 cm long tungsten-alloy cylinder.

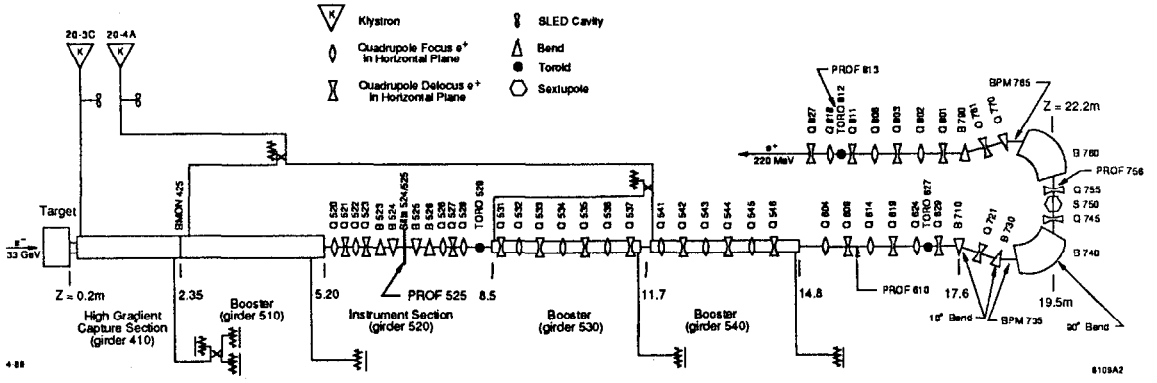

Figure 3. Positron-dedicated linac and initial transport system.

The positrons emerge with a time structure (or bunch length) similar to that of the incident electron bunch ($\sim$ 6 psec). In order to preserve this high-current, short time duration pulse, it would be best to accelerate the beam to relativistic velocities as quickly as possible; however, the positrons also emerge from the target with a small radial extent and large transverse momenta. The positron beam emittance must be matched to the acceptance of the current accelerator capture section, which has a relatively large radial extent but small transverse momentum acceptance. The required phase-space transformation is achieved by immersing the emerging positrons in a quasi-adiabatically decreasing longitudinal magnetic field, which transforms most of their transverse momentum into longitudinal momentum. The decreasing magnetic field is produced by a "flux concentrator" magnet which extends for 10 cm from the downstream edge of the target.

In the current SLC source, the flux concentrator is followed by a 1.5 meter long, high-gradient (30 MeV/meter) accelerator section which accelerates the positrons to 45 MeV. This high-gradient section is followed by a 0.5 meter instrument drift space, and then one 3 meter, low-gradient accelerator section. Next comes a 3 meter instrumentation section in which a magnetic chicane separates the orbit of the positron beam from the electron beam. Beyond this point, profile monitors and current monitors give unambiguous information. This instrument section is followed by two more 3 meter accelerator sections which boost the mean particle energy to 200 MeV—the design energy of the 180° bend magnets that steer the beam into the positron return line.

To understand and optimize positron capture downstream of the target, the dynamics of positrons undergoing acceleration in a sinusoidal longitudinal electric

field must be examined. The change in the particle's energy as a function of position along the central axis is given by

$$\frac{d\gamma}{dz} = -\frac{eE\sin\theta}{m_0c^2}\ , \tag{1}$$

where

m_0c^2 = rest mass energy of positron,
γ = particle energy in units of m_0c^2,
e = charge of the positron,
E = electric field strength,
z = distance along central axis.

The change in the particle's phase with respect to this accelerating field, θ, is given by

$$\frac{d\theta}{dz} = \frac{2\pi}{\lambda}\left(\frac{1}{\beta_W} - \frac{1}{\beta_Z}\right)\ , \tag{2}$$

where

λ = wavelength of the accelerating field,
β_W = velocity of the accelerating wave in units of c,
β_Z = axial positron velocity in units of c.

The solid lines of Fig. 4 represent the longitudinal phase space trajectories of positrons with no transverse momentum undergoing acceleration in a sinusoidal longitudinal electric field. Expressing β_Z in terms of γ and the transverse momentum p_t in units of m_0c, Eqn. 2 becomes

$$\frac{d\theta}{dz} = \frac{2\pi}{\lambda}\left(\frac{1}{\beta_W} - \frac{\gamma}{(\gamma^2 - 1 - p_t^2)^{\frac{1}{2}}}\right)\ . \tag{3}$$

For a velocity of light capture section, β_W=1. If the section is immersed in a uniform axial magnetic field, the transverse momentum, p_t can be considered constant, since the radial RF forces are small. For this case we can integrate Eqns. 1 and 3 yielding

$$\cos\theta_\infty = \cos\theta - \frac{2\pi}{\lambda}\frac{m_0c^2}{eE}\left(\gamma - (\gamma^2 - 1 - p_t^2)^{\frac{1}{2}}\right)\ , \tag{4}$$

which gives the orbits in longitudinal phase space, γ, θ.

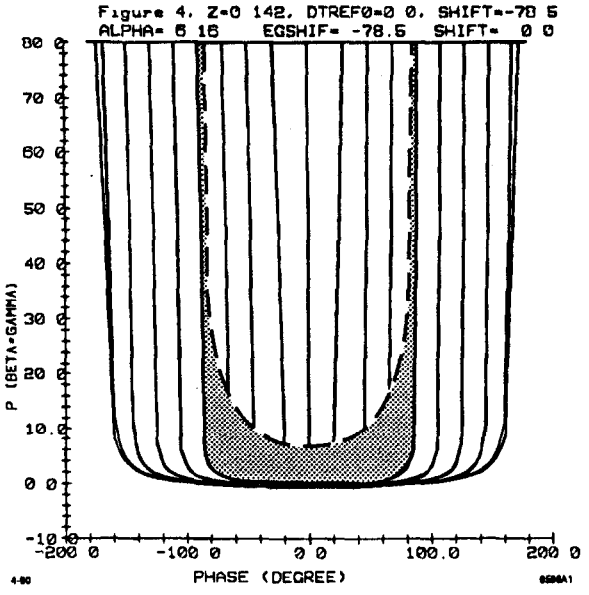

Figure 4. Longitudinal phase space trajectories of positrons with transverse momentum ($0 < p_t < 2m_oc$). The horizontal axis is phase with respect to the accelerating field phase null. The vertical axis is longitudinal momentum in units of m_0c.

Particles whose positions in phase space are on the right side of Fig. 4 are decelerated by the E field until they lag in phase enough to drop behind the field null ($\theta = 0$) and are accelerated. They eventually reach a velocity nearly synchronous with the wave velocity, after which their phase with respect to the wave is constant.

The shaded area represents the phase space trajectories of particles with transverse momenta between 0 and $2m_0c$. Given their higher total momentum for the same longitudinal momentum, they are accelerated less by the E field and therefore follow a trajectory with higher minimum longitudinal momenta.

Figures 5a-e represent the calculated longitudinal emittance of the positron bunch at five positions along the current SLC capture system. Figure 5a represents some 63 e^+/incident e^- emerging from the target with a phase of $\sim$ 3 psec (1 degree at S-band $\sim$ 1 psec). Figure 5b represents the longitudinal emittance of the bunch as it emerges from the flux concentrator. The particle trajectories in the capture system were calculated using the ETRANS ray-tracing code[4]. The lower longitudinal-momentum particles lag in phase because of their smaller longitudinal velocities and their longer (spiral) pathlengths through the flux concentrator. By the end of the flux concentrator, the bunch has a phase extent of $\sim$ 80 psec. Only 8 e^+/e^- arrive at the entrance to the high-gradient accelerator section, where the mean energy is increased to $\sim$ 45 MeV.

At the end of the 9-meter low-gradient accelerator the bunch has a mean energy of $\sim$ 190 MeV (see Figure 5c). A total of 5.3 e^+/e^- reach this point, 90% of which are within the transverse acceptance of the positron return line. About 70% of the

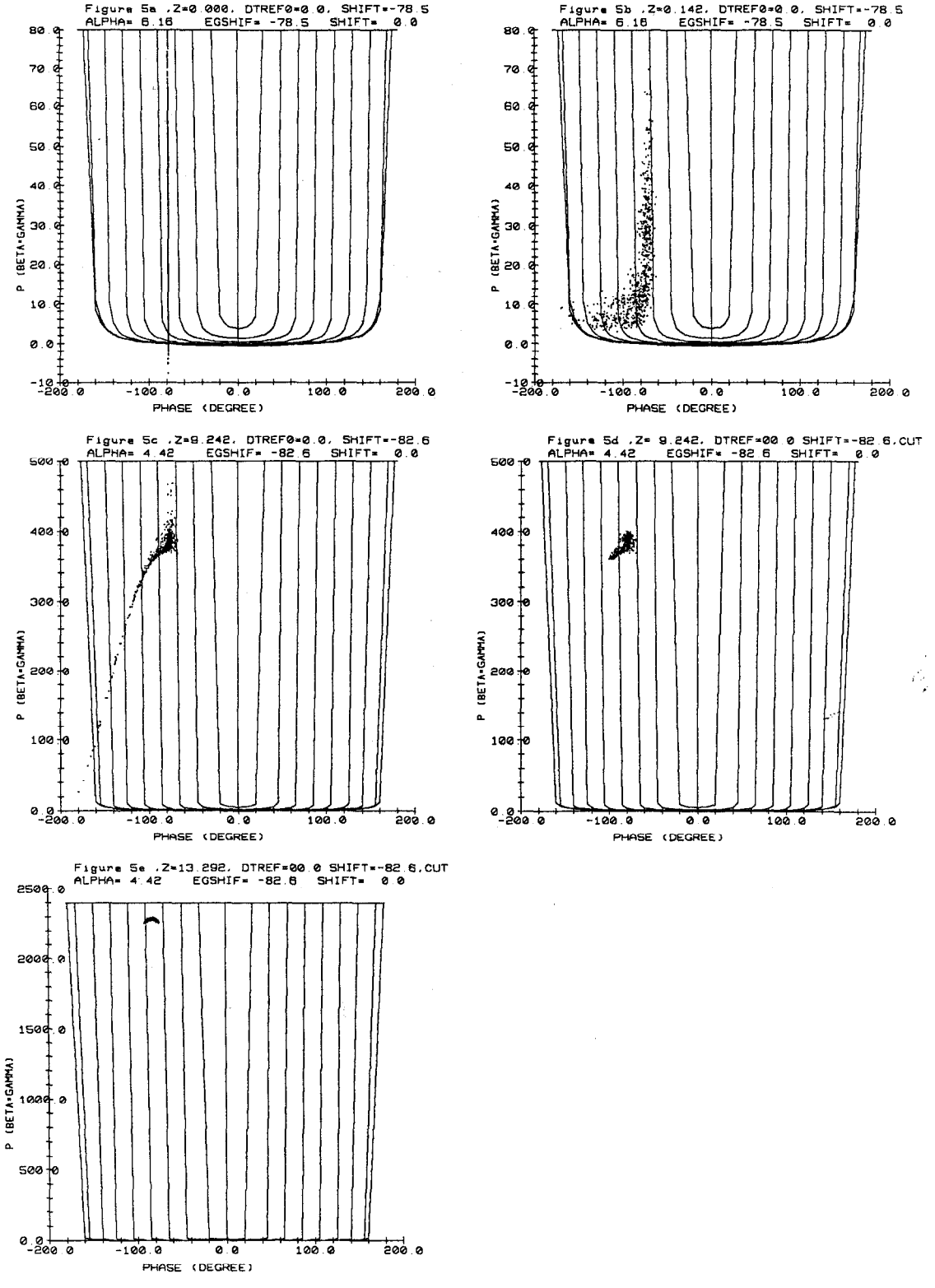

Figure 5. Longitudinal emittance of positron bunch at five positions along the *current SLC* capture system (see text). The vertical smear of points in 5a is direct result of time not being included in the original EGS calculations.

remaining positrons, or 3.5 e^+/e^-, are within the 20 MeV acceptance the 180° return line bends (see Figure 5d). The length of the positron bunch determines its final energy spread at the entrance to the SLC damping rings. The 30 psec bunch length results in a 4% energy spread by the time the positrons are accelerated to 1 GeV at the entrance to the damping ring. As the damping ring acceptance is ±1%, a loss of 25% occurs (see Figure 5e). Thus in the current positron source, ~ 2.5 e^+/e^- arrive at the injection point of the damping ring.

4. Wire Target and New Capture Strategy

Our proposed design combines the higher yield "wire" target with a low-gradient continuous acceleration capture scheme proposed in Ref. 1.

To understand how to optimize the capture in longitudinal phase space, we look at Eqns. 3 and 4. To the second order in $\frac{p_t}{\gamma}$ and $\frac{1}{\gamma}$, Eqn. 3 can be approximated by

$$\frac{d\theta}{dz} = \frac{2\pi}{\lambda}\left(\frac{1}{\beta_W} - \frac{1}{(1-\frac{1}{\gamma^2})^{\frac{1}{2}}} - \frac{p_t^2}{2\gamma^2}\right) . \tag{5}$$

In a drift region γ is constant, and if we let β_W=1, this equation represents the phase lag of a particle with energy γ and normalized transverse momentum p_t relative to a velocity of light particle moving parallel to the axis. In an adiabatically tapered magnetic field, the transverse momentum varies as

$$p_t(z) = p_{t_0}\left(\frac{B(z)}{B_0}\right)^{\frac{1}{2}} .$$

In drifting a distance D between the e^+ target and the accelerator the phase slip relative to a velocity of light particle is

$$\triangle\theta = -\frac{2\pi}{\lambda}\left(\frac{D}{(1-\frac{1}{\gamma_0^2})^{\frac{1}{2}}} + \frac{p_{t_0}^2}{2\gamma_0^2}\frac{1}{B_0}\int_0^D B_z dz\right) .$$

This can also be written as

$$\triangle\theta = -\frac{2\pi}{\lambda}\left(\frac{D}{(1-\frac{1}{\gamma_0^2})^{\frac{1}{2}}} + \frac{p_{t_1}^2}{2\gamma_0^2}K\right) ,$$

where

$$K = \frac{1}{B_1}\int_0^D B_z dz$$

B_1 = the uniform magnetic field in the capture accelerator section,

p_{t_1} = the transverse momentum in the capture section.

Using Eqns. 4 and 6 we can find the condition for two positrons which were created in the target at the same time to have the same asymptotic phase. First, consider two positrons with p_t=0 and different energies, γ_1 and γ_2. They will have the same asymptotic phase if

$$\frac{eE}{m_0c^2}\overline{\sin\theta_{012}} = \frac{1}{D}\left(\frac{\gamma_2\gamma_1}{\gamma_2+\gamma_1}\right) , \tag{7}$$

where $\overline{\sin\theta_{012}}$ is the mean $\sin\theta$ for the two particles as they enter the accelerator sections. Clearly, $\sin\theta$ must be positive which is the region where the particles are decelerated. We can also make the asymptotic phase θ_∞ independent of the transverse momentum for some energy γ_3 chosen to be between γ_1 and γ_2. Using Eqn. 6 to find the phase with which the particles enter the accelerator, and Eqn. 4 to determine their asymptotic phase, we find the condition to be

$$\frac{eE}{m_0c^2}\overline{\sin\theta_{03}} = \frac{1}{K}\frac{\gamma_3^2}{(\gamma_3^2-1)^{\frac{1}{2}}} , \tag{8}$$

where $\overline{\sin\theta_{03}}$ is the mean value of $\sin\theta$ for the two particles entering the structure with differant transverse momenta. Again we find we want to decelerate.

If $\gamma_2 \gg \gamma_1$ (in our case they are 40 and 2 respectively), $\gamma_3^2 \gg 1$, and $\overline{\sin\theta_{012}} \simeq \overline{\sin\theta_{03}}$, we can simplify further and combine Eqns. 7 and 8 to yield

$$\frac{K}{D} \simeq \frac{\gamma_3}{\gamma_1} , \tag{9}$$

$$\frac{eE}{m_0c^2}\overline{\sin\theta_{012}} \simeq \frac{\lambda}{D}\gamma_1 , \tag{10}$$

where $\frac{K}{D}$ is the ratio of the average magnetic field in the flux concentrator (or tapered field solenoid) drift region to the constant magnetic field in the accelerator section. Since we would like to cancel the transverse momentum effect on asymptotic phase near the minimum energy, where it has the largest impact, we want $\frac{K}{D}$ to be as near to unity as possible. This means we must taper down the magnetic field in the flux concentrator as fast as possible, consistent with the large broad-band acceptance in transverse phase space. Secondly, since the left hand side of Eqn. 10 is roughly the rate of acceleration in the capture region, we would like D to be rather small.

Figures 6a-e represent the calculated longitudinal emittance of the positron bunch at five positions along the proposed capture system. Figure 6a represents 195 e^+/e^- emerging from the 1 mm diameter, 10 r.l. wire target. Low-energy positrons emerging from the sides reach the plane of the downstream edge of the target as much as 100 psec behind the first positrons. Figure 6b shows the longitudinal phase space occupied by the positrons which emerge from the flux concentrator. Some 16.5 e^+/e^- occupy a phase extent of $\sim$ 80 psec. Their distribution in phase space is quite similar to that of Figure 5b. Rather than inject this beam into a high-gradient accelerator section, to minimize any further phase spread we chose to inject the beam into a *back-phased, low-gradient* accelerating field. We chose the phase and gradient of the R.F. such that the phase space occupied by the beam lay along the "contour lines" of the particle orbits as shown in Figure 6b. The beam's subsequent trajectory in phase space results in the smallest possible asymptotic phase spread.

In order for this strategy to work the positrons must be uniformly accelerated with no drift sections until all the positrons have energies greater than or equal to 10 MeV. Since some positrons are decelerated from 20 MeV down to low energy and then are reaccelerated, this takes about 30 MeV of acceleration, or about 3 meters of the low gradient accelerator. Thus, for this strategy, we eliminate the 0.5 meter instrumentation section. This section serves little purpose since both electrons and positrons are in the beam at this point.

Figures 6c-e illustrate the motion of the beam as it traverses the 5 meter low-gradient (E = 12 MeV/meter) accelerator (Figure 6c), followed by 6 meters of high-gradient (E = 29 MeV/meter) accelerator (Figures 6d-e). We propose to replace the quadrupole focusing on the final six meter accelerator section with solenoidal focusing, which eliminates losses due to the present transverse acceptance at the entrance to this structure. We find that 9.5 e^+/e^- arrive at the end of the 6 meter low-gradient structure with a phase extent of $\sim$ 15 psec. Note that most of the positrons are initially *decelerated*, yet the final phase spread of the beam is significantly less than that of the present source.

Because of the reduced phase extent of the beam at the 190 MeV point, only 2% are lost in the 180° bend leading to the positron return line. The 15 psec bunch length is small enough to accelerate all particles to 1 GeV within the 1% energy acceptance of the damping ring.

Our simulations predict that 9.3 e^+/e^- can be produced within a suitable phase space for damping ring acceptance—more than tripling the present yield.

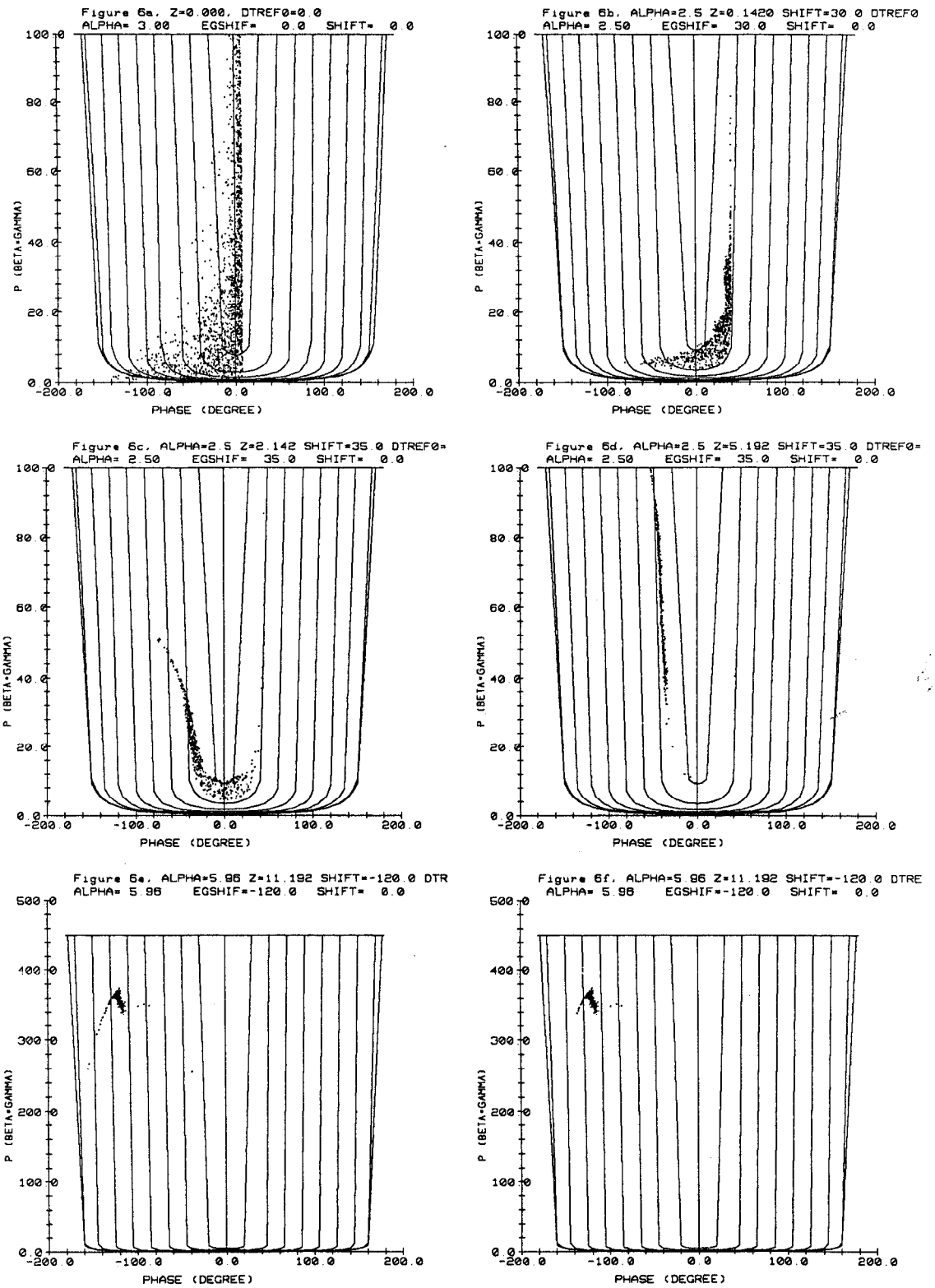

Figure 6. Longitudinal emittance of positron bunch at six positions along the *proposed* capture system (see text).

5. Summary of Results

Since it is possible to upgrade the target and capture system separately, we divided up the simulations as follows:

1. The production of positrons by the *wire target*, but injected into the *current capture system.*
2. The production of positrons by the *current target*, but injected into the *proposed capture system.*

The results for all four combinations are summarized in Figure 7 and Table 1.

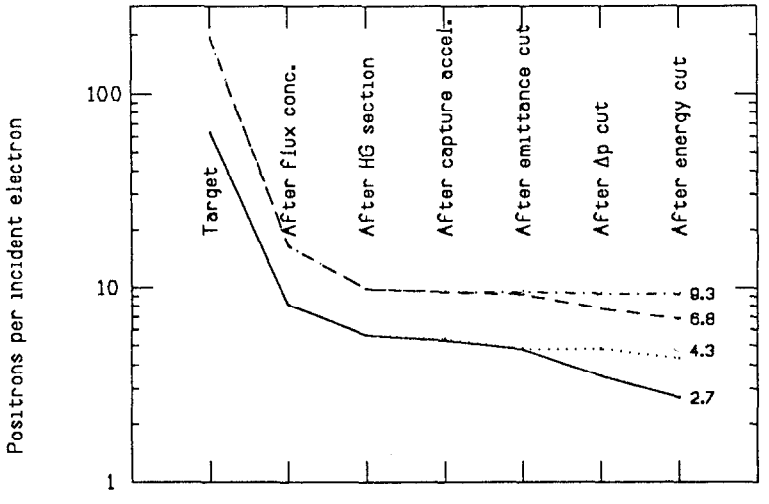

Figure 7. Positron yields at various stages of capture for the four combinations discussed in the text.

Table 1. Summary of Target Yields (e^+/e^-).

	Slab Target	Wire Target
Present Capture	2.7	6.8
New Capture	4.3	9.3

6. Conclusions

Monte Carlo simulation of positron yields from wire targets have been presented that demonstrate that the current positron production and capture system of the SLC might be improved with existing hardware, possibly tripling the current yield.

Further work includes additional simulations with EGS4 to explore shaping the target to obtain the highest possible photon track length, and including recent[5] low-energy enhancements to EGS4. Further study of the capture system is needed to explore possible improvements in the transverse phase space capture. In particular, we wish to explore the possibility of immersing the down stream end of the target in the field of the flux concentrator to reduce loss of positrons emitted from the sides of the target. Additional study is also required to understand and realize suitable mechanical properties of the wire target including strength, heat transfer, and durability.

REFERENCES

1. B. Aune, R. H. Miller: "New Method for Positron Production at SLAC", proceedings of the 1979 Linear Accelerator Conference, Montauk, N.Y., Sept. 10-14 (1979).
2. W. R. Nelson, H. Hirayama and D. W. O. Rogers: "The EGS4 Code System", Stanford Linear Accelerator Center report SLAC-265 (1985).
3. J. E. Clendenin, "High-Yield Positron Systems for Linear Colliders", presented at the IEEE Particle Accelerator Conference, Chicago, 20-23 March 1989; SLAC-PUB-4743 (1989).
4. H. L. Lynch, "Documentation of ETRANS Program", SLAC internal memo to the SLC Positron Source Group (27 October 1988).
5. T. M. Jenkins, W. R. Nelson and A. Rindi, *Monte Carlo Transport of Electrons and Photons* (Plenum Press, 1988).